Kinetics and Thermodynamics of Formation of Copper–Dioxygen Adducts: Oxygenation of Mononuclear Copper(I) Complexes Containing Tripodal Tetradentate Ligands

Kenneth D. Karlin,*,† Ning Wei,† Bernhard Jung,‡ Susan Kaderli,‡ Pascal Niklaus,‡ and Andreas D. Zuberbühler*,‡

Contribution from the Department of Chemistry, The Johns Hopkins University, Baltimore, Maryland 21218, and Institute of Inorganic Chemistry, University of Basel, CH-4056 Basel, Switzerland

Received May 4, 1993®

Abstract: Copper–dioxygen (O_2) interactions are of interest in chemical as well as biological transformations involving reversible O_2-binding, oxygenation, or oxidation of organic substrates. In this report, we describe the complete kinetics and thermodynamics of O_2-reactions with a series of mononuclear copper(I) complexes containing N_4-tripodal tetradentate donor ligands. The latter include tris[(2-pyridyl)methyl]amine (TMPA) and corresponding ligands with one (BPQA), two (BQPA), or three (TMQA) 2-quinolyl groups substituting for 2-pyridyl donors. $[(TMPA)Cu(CH_3CN)]^+$ (**1a**) is known to react with O_2 in EtCN or CH_2Cl_2 at −80 °C to form a dinuclear (II) complex, $[\{(TMPA)Cu\}_2(O_2)]^{2+}$ (**1c**), with a *trans*-μ-1,2-peroxo dicopper(II) structure, as determined by X-ray crystallography (Tyeklár, Z.; et al. *J. Am. Chem. Soc.* **1993**, *115*, 2677–2689). $[(BPQA)Cu]^+$ (**2a**) and $[(BQPA)Cu]^+$ (**3a**) also form O_2-adducts, but $[(TMQA)Cu]^+$ (**4a**) is unreactive. Variable-temperature (−90 °C to room temperature), multiwavelength (359–776 nm), stopped-flow data were collected. The numerical analysis shows that all three reacting Cu(I) species **1a**–**3a** follow the same reaction mechanism, involving the initial reversible formation (k_1/k_{-1}) of 1:1 Cu:O_2 adducts $[LCu(O_2)]^+$ (**1b**–**3b**), which react reversibly (k_2/k_{-2}) with starting Cu(I) species **1a**–**3a** to form 2:1 complexes $[(LCu)_2(O_2)]^{2+}$ (**1c**–**3c**), respectively. However, considerable differences exist in detail, depending on the ligand. Thus, the 1:1 adduct **1b** ($k_1 = 2 \times 10^4$ M^{-1} s^{-1}, $K_1 = k_1/k_{-1} = 1.9 \times 10^3$ M^{-1} at −90 °C) is observed spectroscopically below −70 °C (λ_{max} = 410 nm, ϵ = 4000 M^{-1} cm^{-1}) prior to the transformation ($k_{ter} = k_1k_2/k_{-1} = 6 \times 10^7$ M^{-2} s^{-1}, −90 °C) to the final stable dinuclear product **1c**. In the reaction of $[(BPQA)Cu]^+$ (**2a**) with O_2, the 1:1 intermediate was not observable and the stable 2:1 adduct $[\{(BPQA)Cu\}_2(O_2)]^{2+}$ (**2c**) formed rapidly, having spectroscopic properties very similar to those for **1c**. In the case of $[(BQPA)Cu]^+$ (**3a**), both 1:1 and 2:1 adducts formed and were spectroscopically characterized. Here, the thermodynamically stable product is the 1:1 adduct $[\{(BQPA)Cu\}(O_2)]^+$ (**3b**) (λ_{max} = 378 nm, ϵ = 8000 M^{-1} cm^{-1}; $k_1 = 18$ M^{-1} s^{-1}, $K_1 = k_1/k_{-1} = 3 \times 10^3$ M^{-1} at −90 °C), but the kinetics are such that there is an "overshoot", and the 2:1 adduct $[\{(BQPA)Cu\}_2(O_2)]^+$ (**3c**) forms initially (λ_{max} = 545 nm, ϵ = 5500 M^{-1} cm^{-1}) as an intermediate. The temperature-dependent data allow for thermodynamic analyses, showing that Cu_nO_2 (n = 1 or 2) bonding is strong at reduced temperatures with favorable negative enthalpies, $\Delta H° \simeq -34$ kJ mol^{-1} for 1:1 adducts and −50 to −80 kJ mol^{-1} for 2:1 adducts. However, room-temperature instabilities are caused by strongly negative reaction entropies, $\Delta S° \simeq -200$ J K^{-1} mol^{-1}, for 2:1 adducts. The kinetic and thermodynamic parameters are compared with corresponding data for cobalt(II)– and iron(II)–porphyrin complexes as well as that for iron and copper proteins. The synthetic copper–dioxygen adducts form with rate constants comparable to or exceeding those of iron and cobalt, and the present investigation shows that Cu/O_2 interactions can indeed be studied in detail.

Introduction

A detailed understanding of dioxygen (O_2; molecular oxygen) interactions with transition metals is important in a variety of synthetic, industrial, and biological processes.[1-10] The binding of dioxygen to iron and cobalt has been intensively studied, in large part because of the biological occurrence of important hemoproteins such as myoglobin and hemoglobin, relevant model compounds, and cobalt analogues.[6-11] Compared to those metal ions, copper-containing systems are less well-understood, in spite of the fact that they mediate very similar kinds of biological or chemical reactions.[12-14] Copper–dioxygen interactions occur in proteins such as hemocyanin (O_2-carrier)[15-18] and monooxy-

† The Johns Hopkins University.
‡ University of Basel.
* Address for correspondence: Professor K. D. Karlin, Department of Chemistry, The Johns Hopkins University, 3400 N. Charles St., Baltimore, MD 21218.

® Abstract published in *Advance ACS Abstracts*, September 15, 1993.

(1) *Oxygen Complexes and Oxygen Activation by Transition Metals*; Martell, A. E., Sawyer, D. T., Eds.; Plenum: New York, 1988.
(2) Gubelmann, M. H.; Williams, A. F. *Struct. Bonding (Berlin)* **1983**, *55*, 1–65.
(3) *Dioxygen Activation and Homogeneous Catalytic Oxidation*; Simándi, L. I., Ed.; Elsevier Science Publishers B. V.: Amsterdam, 1991; Vol. 66.
(4) *Activation and Functionalization of Alkanes*; Hill, C. L., Ed.; Wiley-Interscience: New York, 1989.
(5) Sheldon, R. A.; Kochi, J. M. *Metal-Catalyzed Oxidations of Organic Compounds*; Academic Press: New York, 1981.
(6) Dawson, J. H. *Science* **1988**, *240*, 433–439.
(7) Niederhoffer, E. C.; Timmons, J. H.; Martell, A. E. *Chem. Rev.* **1984**, *84*, 137–203.
(8) Fallab, S.; Mitchell, P. R. *Adv. Inorg. Bioinorg. Mech.* **1984**, *3*, 311–377.
(9) *Metal Ion Activation of Dioxygen: Metal Ions in Biology*; Spiro, T. G., Ed.; Wiley-Interscience: New York, 1980; Vol. 2.
(10) Jones, R. D.; Summerville, D. A.; Basolo, F. *Chem. Rev.* **1979**, *2*, 139–179.
(11) Ingraham, L. I.; Meyer, D. L. In *Biochemistry of the Elements*; Frieden, E., Ed.; Plenum Press: New York, 1985; Vol. 4.
(12) *Bioinorganic Chemistry of Copper*; Karlin, K. D., Tyeklár, Z., Eds.; Chapman & Hall: New York, 1993.
(13) Karlin, K. D.; Tyeklár, Z.; Zuberbühler, A. D. In *Bioinorganic Catalysis*; Reedijk, J., Ed.; Marcel Dekker: New York, 1993; pp 261–315.
(14) Kitajima, N. *Adv. Inorg. Chem.* **1992**, *39*, 1–77.
(15) Volbeda, A.; Hol, W. G. J. *J. Mol. Biol.* **1989**, *209*, 249–279.

0002-7863/93/1515-9506$04.00/0

genases including tyrosinase (*ortho*-hydroxylation of phenols),[16] dopamine β-hydroxylase,[19,20] and phenylalanine hydroxylase[21,22] as well as oxidases (e.g., O_2 reduction to H_2O or H_2O_2) such as laccase,[16] ascorbate oxidase,[16,23] galactose oxidase,[24,25] amine oxidases,[26] and the iron–copper-containing cytochrome *c* oxidase.[27,28]

As part of an overall program to elucidate basic coordination chemistry relevant to biological and chemical utilization of O_2, we have been carrying out biomimetic Cu^I_n/O_2 reactivity investigations.[13,29] Kinetic and thermodynamic studies have been a part of these efforts, since very limited data are available on either copper proteins or model compounds.[13,30,31]

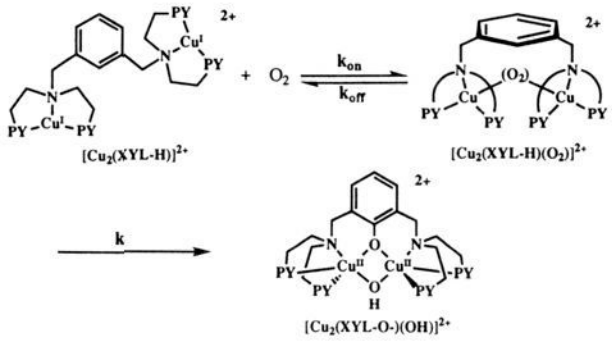

In fact, a tyrosinase model system we have described[13,32] ($[Cu_2(XYL–H)]^{2+} + O_2 \rightarrow [Cu_2(XYL–O–)OH]^{2+}$) is unique for its complete kinetic/thermodynamic description of both the reversible O_2-binding step and the subsequent hydroxylation.[13,31]

Another chemical system that has thus far provided particular insights is the mononuclear copper(I) complex containing the tripodal tetradentate ligand tris[(2-pyridyl)methyl]amine (TMPA).[33–35] The mononuclear complex $[(TMPA)Cu(RCN)]^+$ (**1a**) undergoes a reversible reaction with dioxygen to form a Cu_2O_2 complex, one that we were able to characterize by X-ray crystallography.[33,35] The product $[\{(TMPA)Cu\}_2(O_2)]^{2+}$ (**1c**) contains a *trans*-μ-1,2-peroxo-bridged dicopper(II) moiety, with

Chart I

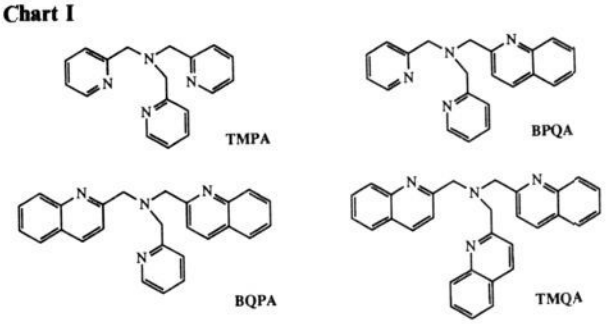

	[(TMPA)Cu(RCN)]+	[(BPQA)Cu]+	[(BQPA)Cu]+	[(TMQA)Cu]+
$[LCu]^+$	**1a**	**2a**	**3a**	**4a**
$[LCuO_2]^+$	**1b**	**2b**	**3b**	
$[(LCu)_2O_2]^{2+}$	**1c**	**2c**	**3c**	

Cu···Cu = 4.36 Å. The overall formation of this $Cu_2O_2^{2+}$ complex **1c** from **1a** and dioxygen is shown.

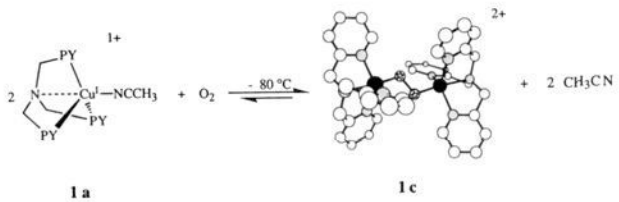

1a **1c**

We have previously examined Cu(I) and Cu(II) complexes with tripodal tetradentate ligands possessing different donor groups (e.g., pyridine vs thioether)[36,37] or variable chelate ring size[38–40] and have observed dramatic effects upon structure, redox potential, or reactivity of the respective complexes.[36–44] As an extension of the study of the $[(TMPA)Cu(RCN)]^+/O_2$ interaction, we have also been looking at quinolyl-containing copper(I) analogues $[LCu]^+$ (**2a–4a**), where L = BPQA, BQPA, and TMQA as shown in Chart I.[44] We expected that substitution of 2-quinolyl for 2-pyridyl donors might influence the O_2-binding process for steric reasons, while these changes might also alter O_2-reactivity because of an effect upon the inherent LCu(II)/LCu(I) redox potentials. In fact, we do find that quinolyl-containing analogues possess a more positive redox potential.[44] In this report, we describe and compare the complete kinetics/thermodynamics of O_2-interaction of **1a–4a**. In our preliminary study of $[(TMPA)Cu(RCN)]^+$ (**1a**),[30] an exciting finding was that at low temperature, an intermediate, the Cu–O_2 1:1 adduct $[\{(TMPA)Cu\}(O_2)]^+$ (**1b**), could be detected and the investigation thus revealed the first description of a primary copper–dioxygen 1:1 adduct.

Experimental Section

Materials and Methods. Reagents and solvents used were of commercially available reagent quality unless otherwise stated. Propionitrile (Merck) was treated prior to use to remove impurities and water by

(16) Solomon, E. I.; Baldwin, M. J.; Lowery, M. D. *Chem. Rev.* **1992**, *92*, 521–542.
(17) Magnus, K.; Ton-That, H. *J. Inorg. Biochem.* **1992**, *47*, 20.
(18) Hazes, B.; Magnus, K. A.; Bonaventura, C.; Bonaventura, J.; Dauter, Z.; Kalk, K.; Hol, W. G. J. *Protein Science* **1993**, *2*, 597–619.
(19) Klinman, J. P.; Berry, J. A.; Tian, G. In *Bioinorganic Chemistry of Copper*; Karlin, K. D., Tyeklár, Z., Eds.; Chapman & Hall: New York, 1993; pp 151–163.
(20) Stewart, L. C.; Klinman, J. P. *Ann. Rev. Biochem.* **1988**, *57*, 551–592.
(21) Pember, S. O.; Johnson, K. A.; Villafranca, J. J.; Benkovic, S. J. *Biochemistry* **1989**, *28*, 2124–2130.
(22) Dix, K. A.; Benkovic, S. J. *Acc. Chem. Res.* **1988**, *21*, 101–107.
(23) Messerschmidt, A. In *Bioinorganic Chemistry of Copper*; Karlin, K. D., Tyeklár, Z., Eds.; Chapman & Hall: New York, 1993; pp 471–484.
(24) Ito, N.; Phillips, S. E. V.; Stevens, C.; Ogel, Z. B.; McPherson, M. J.; Keen, J. N.; Yadav, K. D. S.; Knowles, P. F. *Nature* **1991**, *350*, 87–90.
(25) Whittaker, J. W. In *Bioinorganic Chemistry of Copper*; Karlin, K. D., Tyeklár, Z., Eds.; Chapman & Hall: New York, 1993; pp 447–458.
(26) Dooley, D. M.; McGuirl, M. A.; Brown, D. E.; Turowski, P. N.; McIntire, W. S.; Knowles, P. F. *Nature* **1991**, *349*, 262–264.
(27) Babcock, G. T.; Wilkström, M. *Nature* **1992**, *356*, 301–309.
(28) Fee, J. A.; Antholine, W. E.; Fan, C.; Gurbiel, R. J.; Surerus, K.; Werst, M.; Hoffman, B. M. In *Bioinorganic Chemistry of Copper*; Karlin, K. D., Tyeklár, Z., Eds.; Chapman & Hall: New York, 1993; pp 485–500.
(29) Karlin, K. D.; Tyeklár, Z. In *Bioinorganic Chemistry of Copper*; Karlin, K. D., Tyeklár, Z., Eds.; Chapman & Hall: New York, 1993; pp 277–291.
(30) Karlin, K. D.; Wei, N.; Jung, B.; Kaderli, S.; Zuberbühler, A. D. *J. Am. Chem. Soc.* **1991**, *113*, 5868–5870.
(31) Cruse, R. W.; Kaderli, S.; Karlin, K. D.; Zuberbühler, A. D. *J. Am. Chem. Soc.* **1988**, *110*, 6882–6883.
(32) Nasir, M. S.; Cohen, B. I.; Karlin, K. D. *J. Am. Chem. Soc.* **1992**, *114*, 2482–2494.
(33) Jacobson, R. R.; Tyeklár, Z.; Karlin, K. D.; Liu, S.; Zubieta, J. *J. Am. Chem. Soc.* **1988**, *110*, 3690–3692.
(34) Baldwin, M. J.; Ross, P. K.; Pate, J. E.; Tyeklár, Z.; Karlin, K. D.; Solomon, E. I. *J. Am. Chem. Soc.* **1991**, *113*, 8671–8679.
(35) Tyeklár, Z.; Jacobson, R. R.; Wei, N.; Murthy, N. N.; Zubieta, J.; Karlin, K. D. *J. Am. Chem. Soc.* **1993**, *115*, 2677–2689.
(36) Karlin, K. D.; Dahlstrom, P. L.; Hyde, J. R.; Zubieta, J. *J. Chem. Soc., Chem. Commun.* **1980**, *906*, 906–908.
(37) Karlin, K. D.; Yandell, J. K. *Inorg. Chem.* **1984**, *23*, 1184–1188.
(38) Karlin, K. D.; Hayes, J. C.; Juen, S.; Hutchinson, J. P.; Zubieta, J. *Inorg. Chem.* **1982**, *21*, 4106–4108.
(39) Zubieta, J.; Karlin, K. D.; Hayes, J. C. In *Copper Coordination Chemistry: Biochemical and Inorganic Perspectives*; Karlin, K. D., Zubieta, J., Eds.; Adenine Press: Albany, NY, 1983; pp 97–108.
(40) Jacobson, R. R. Ph.D. Dissertation Thesis, State University of New York (SUNY) at Albany, 1989.
(41) Karlin, K. D.; Hayes, J. C.; Hutchinson, J. P.; Hyde, J. R.; Zubieta, J. *Inorg. Chim. Acta* **1982**, *64*, L219–L220.
(42) Karlin, K. D.; Sherman, S. E. *Inorg. Chim. Acta* **1982**, *65*, L39–L40.
(43) Augustin, M. A.; Yandell, J. K.; Addison, A. W.; Karlin, K. D. *Inorg. Chim. Acta* **1981**, *55*, L35.
(44) Wei, N.; Tyeklár, Z.; Karlin, K. D. Manuscript in preparation.

drying with phosphorus pentoxide (P_2O_5) and distilling under normal pressure. It was then kept dry by storing over calcium hydride (Merck) in a closed system which was composed of a brown, round-bottom flask and a specially made condenser.[45] The dioxygen-free propionitrile was collected under reduced pressure and handled strictly under a nitrogen atmosphere by using a vacuum line.

Copper(I) Complex Solution. Yellow, dioxygen-sensitive samples of **1a**,[35] **2a**,[44] and **3a**[44] were stored in glass vials under argon. A glovebox was used to transfer these compounds into an addition funnel modified for air-sensitive manipulations.[45] Freshly distilled propionitrile was carefully transferred to the addition funnel under nitrogen, and the complex solution was then ready for use.

Dioxygen/Air Solution. Propionitrile, saturated with dioxygen or air, was prepared by passing dried O_2 or air through the solvent for 20 min. The stopcocks were then closed, and the gas-saturated solvent was equilibrated in a 25 °C water bath. After equilibration, any pressure inside the addition funnel was released by briefly opening the stopcock. The addition funnel containing the O_2- or air-saturated solution was then put on the stopped-flow instrument.

During the whole series of measurements, nitrogen and dioxygen or air were purged slowly through tubes connected with the two addition funnels containing the copper(I) complex and dioxygen/air solutions, respectively.

O_2-Solubility in Propionitrile. The solubility of dioxygen in propionitrile was determined by using an oxygen-sensitive Clark electrode. A small amount of air-saturated solvent was added to deaerated, twice-distilled water, and the change in dioxygen concentration was monitored. The calculation was based on the O_2-solubility of 1.245×10^{-3} M in water.[46] The average value of the O_2-solubility of $(8.8 \pm 1.0) \times 10^{-3}$ M atm^{-1} in propionitrile was calculated on the basis of eight measurements. The O_2 content of 1.8×10^{-3} M in air-saturated propionitrile was calculated on the basis of 21% O_2 present in air.

Density of Propionitrile. We thank Professor Dr. H. Weingärtner, University of Karlsruhe (Germany), for the density data of propionitrile in the range of 0–50 °C. Together with our own values in the range of −86 to 0 °C, the density of propionitrile could be very satisfactorily described by a linear equation: d (g/cm^3) = 0.8011 ± 0.0004 − (9.801 ± 0.090) × 10^{-4} × T, where T is the temperature in °C. This relation was used to calculate concentrations at various temperatures, based on a given solution kept at room temperature in the addition funnel.

Stopped-Flow Instrument and Software. The SFL-21 (2-mm light path/2-mL syringes) low-temperature flow unit of a SF-3A stopped-flow system (Hi-Tech Scientific) was coupled to a Zeiss MCS 512 diode array detector using flexible light guides. The two glass coils, containing Cu(I) and oxygen solutions, respectively, and the mixing chamber were immersed in an ethanol bath. This bath was placed in a dewar, which was filled with liquid nitrogen for low-temperature measurements. The ethanol bath was cooled by liquid nitrogen evaporation, and its temperature was measured by using a Pt resistance thermometer and maintained to ±0.1 K by using a temperature-controlled thyristor power unit (both Hi-Tech). Complete spectra were collected between 359 and 776 nm. Data collected from stopped-flow measurements were transferred from the Zeiss asynchrone port to a Hewlett-Packard 300 desk computer through a self-built DMA interface based on a HP-98360 Bread Board interface card with 74LS04, 74LS32, and 74LS221 chips and a specifically written subroutine in assembler language.[47] The data were compressed by factor analysis[48,49] and stored in their eigenvector representations as described before for spectrophotometric equilibrium data.[50] They were then transferred and analyzed on an IBM PC/AT by the computer pogram KINFIT.[51]

Data Reduction Methods. KINFIT allows the fitting of various selected models to the eigenvector representations of spectrophotometric kinetic data. Kinetic (rate constants) and thermodynamic (equilibrium constants) parameters may be equally introduced and given fixed or adjustable values. Also, spectra of the absorbing species may be either specified and kept constant on the basis of independent measurements or adjusted and refined in the iterative process.

Due to the wide range of bimolecular rate constants involved, concentration–time profiles had to be calculated by numerical integration, using a routine for stiff differential equations.[52] Refinement of rate and equilibrium constants was based on the algorithm proposed by Marquardt[53] in order to assure convergence of the iterative process. Unknown spectra were replaced by their linear least-squares estimates in the eigenvector space during the iterative process as described previously for spectrophotometric data.[50]

In some cases, it was advisable or even necessary to keep certain spectra fixed at values determined independently. This need arises specifically in the cases of incompletely formed species or of rapid preequilibria. In the latter case, factor analysis of the kinetic data does not always yield a satisfactory representation of the space spanned by the real spectra and the eigenvector basis had to be appropriately enhanced by including the original known spectra into the set used for factor analysis. This transformation of the eigenvector basis may be routinely achieved by KINFIT.

A third routine of KINFIT allows the direct calculation of equilibrium concentrations and thus of thermodynamic parameters on the basis of a single experimental spectrum and the known spectra of all species involved in the equilibrium mixture. Writing Beer's law as $\epsilon \cdot \mathbf{C} = \mathbf{A}$, we obtained column vector $\mathbf{C}$ of the concentrations by simple linear regression as $\mathbf{C} = (\epsilon^t\epsilon)^{-1}\epsilon^t\mathbf{A}$, where ϵ represents the matrix of the known species spectra and $\mathbf{A}$ the column vector of the measured absorbances. This approach was necessary for the preanalysis of the TMPA data at all but the lowest temperatures. In addition, equilibrium concentrations and equilibrium constants were calculated directly (i.e., from UV–vis spectra) on the basis of incomplete formation of one of the products when appropriate, e.g., for the calculation of K_2 at higher temperatures.

Kinetic Measurements. For [(TMPA)Cu(RCN)]$^+$ (**1a**), five series of Cu(I) concentrations were used to carry out a total of 132 measurements (three series reacted with the oxygen-saturated propionitrile solution and two series reacted with the air-saturated propionitrile solution) which were used for the final calculations. The concentrations of Cu(I) solutions used were $(1.92–6.59) \times 10^{-4}$ M. The temperature was varied between −90 and −12 °C, and the data collection time ranged from 0.3 to 4 s.[30]

For [(BPQA)Cu]$^+$ (**2a**), five series of Cu(I) concentrations were used to carry out a total of 153 measurements (four series reacted with the oxygen-saturated solution and one series reacted with the air-saturated solution) which were used for the final calculations. The Cu(I) concentrations were $(2.02–9.57) \times 10^{-4}$ M. The temperature was varied between −90 and −25 °C, and the data collection time ranged typically from 0.5 to 10 s. Longer collection times up to 120 s were used in attempting to study the secondary decay of the 2:1 adduct; these latter results are not discussed in this report.

For [(BQPA)Cu]$^+$ (**3a**), three series of Cu(I) concentrations were used to carry out a total of 80 measurements (all reacted with the oxygen-saturated solution) which were used for the final calculations. The concentrations of Cu(I) solutions used were $(5.0–9.6) \times 10^{-4}$ M. Spectra were taken in the temperature range of −90 to −70 °C. The data collection time ranged from 2 to 120 s.

Low-Temperature UV–Vis Spectroscopy and Molar Absorptivity of [{(BQPA)Cu}(O_2)]$^+$ (3b). Low-temperature spectrophotometric studies were also carried out on a Hewlett-Packard 8452A diode array spectrophotometer driven by a Compaq Deskpro 386S computer using software written by On Line Instrument Systems (OLIS) Inc. with output to an Okidata Microline 320 printer. The sample compartment was modified for low-temperature manipulations. A Kontes KM-611772 variable-temperature UV–vis Dewar cell fitted with quartz windows was mounted on a specially constructed stand. The cuvette assembly consisted of a 10-mm quartz cuvette fused to one end of a glass tube; the other end was attached to a high-vacuum stopcock and a 14/20 ground-glass joint as previously described.[54,55] To maintain a low temperature, a copper

(45) We thank R. Cruse for the design of this setup. Detailed drawings of the apparatus are available with the supplementary material.

(46) *Handbook of Chemistry and Physics*, 62nd ed.; Astle, M. J., Weast, R. C., Eds.; CRC Press: Boca Raton, FL, 1981–1982.

(47) We thank C. J. Meyer for the construction of the DMA interface using a Hewlett-Packard 98630 bread Board. An outlay of the DMA interface and listings of the assembler program are available with the supplementary material.

(48) Malinowkski, E. R.; Howery, D. G. *Factor Analysis in Chemistry*; Wiley-Interscience: New York, 1980.

(49) Delaney, M. F. *Anal. Chem.* **1984**, *56*, 261R.

(50) Gampp, H.; Maeder, M.; Meyer, C. J.; Zuberbühler, A. D. *Talanta* **1985**, *32*, 95–110.

(51) Jung, B.; Zuberbühler, A. D. To be published. This is a modified version of the program originally developed for data reduction directly on the HP 300 computer. (Cruse, R. W.; Kaderli, S.; Mayer, C. J.; Zuberbühler, A. D.; Karlin, K. D. *J. Am. Chem. Soc.* **1988**, *110*, 5020–5024.)

(52) Gear, C. W. *Numerical Initial Value Problem in Ordinary Differential Equations*; Prentics Hall: Englewood Cliffs, NJ, 1971.

(53) Marquardt, D. W. *J. Ind. Appl. Math.* **1963**, *11*, 431–441.

(54) Karlin, K. D.; Haka, M. S.; Cruse, R. W.; Meyer, G. J.; Farooq, A.; Gultneh, Y.; Hayes, J. C.; Zubieta, J. *J. Am. Chem. Soc.* **1988**, *110*, 1196–1207.

tubing coil was inserted into the methanol-filled dewar, through which cold methanol was circulated from an external source (Neslab CC-100 cryocool immersion cooler in Agitainer A with circulating pump). Temperatures in the dewar and the Agitainer were monitored by using resistance thermocouple probes (Omega Models 651 and 650, respectively). To obtain the molar absorptivity at –80 °C for **3b**, low-temperature UV–vis spectra were taken. The sample solutions were prepared in a cuvette assembly which had been precalibrated for volume vs height. Before the sample was prepared, a background scan with pure solvent was taken. Solid **3a** was placed into the cuvette assembly under argon, and dried propionitrile was then directly distilled into it. The cuvette assembly was then cooled in a liquid N_2/methanol bath (–80 °C), and the height was noted ($[LCu]^+ = 10^{-4}$–10^{-3} M). After placing the cuvette into the dewar, the Cu(I) spectrum was recorded. The solution was then oxygenated by directly bubbling dry dioxygen through it for 1–2 min. The maximum absorbance observed at 378 nm was used to calculate its molar absorptivity ϵ. The average ϵ value obtained was 8200 M^{-1} cm^{-1}.

Results and Discussion

Mechanism for the Oxygenation Reaction of Copper(I) Complexes 1a–4a. As $[\{(TMPA)Cu\}_2(O_2)]^{2+}$ (**1c**) has been fully characterized by X-ray crystallography, it offers an excellent opportunity to study its kinetics and thermodynamics. We recently reported that the interaction of $[(TMPA)Cu(RCN)]^+$ (**1a**) with dioxygen follows the reaction mechanism shown in Scheme I.[30] From the present extended kinetic study on the

Scheme I

$$\underset{\mathbf{1a}}{[LCu(RCN)]^+} + O_2 \underset{k_{-1}}{\overset{k_1}{\rightleftharpoons}} \underset{\mathbf{1b}}{[LCu(O_2)]^+} + RCN \qquad (1)$$

$$\underset{\mathbf{1a}}{[LCu(RCN)]^+} + \underset{\mathbf{1b}}{[LCu(O_2)]^+} \underset{k_{-2}}{\overset{k_2}{\rightleftharpoons}} \underset{\mathbf{1c}}{[(LCu)_2(O_2)]^{2+}} + RCN \qquad (2)$$

$$\underset{\mathbf{1c}}{[(LCu)_2(O_2)]^{2+}} \rightarrow \text{irreversible decay} \qquad (3)$$

reaction of mononuclear Cu(I) complexes **1a–4a** with dioxygen, we find that the copper(I) complexes **1a–3a** interact quasi-reversibly with O_2 and the same basic reaction mechanism can be applied. At low temperature, one mononuclear $[LCu]^+$ ion first reacts in a reversible fashion with a dioxygen molecule to form a 1:1 Cu–O_2 species; the latter further reacts reversibly with a second $[LCu]^+$ ion to form the final dinuclear 2:1 Cu_2O_2 adduct. Although these three copper(I) systems interact with dioxygen according to the same reaction mechanism, their behavior differs considerably in detail. The relative stabilities of the two copper–dioxygen species (i.e., 1:1 or 2:1 adducts) depend on the ligand. Also, the accumulation of either of the two copper–dioxygen species depends on their equilibrium constants and on the rate constants for the individual steps.

Calculations for the present kinetic experiments are based on the reaction mechanism (Scheme I), with one or more simplifications depending on the experimental observations. Some of the kinetic parameters can only be calculated in a restricted temperature range, and outside the range, either extrapolated values may have to be used or the mechanistic model scheme may be appropriately simplified. From the temperature dependence of the individual rate and equilibrium constants, activation parameters as well as reaction enthalpies and entropies were obtained for all experimentally accessible parameters. These values represent the fundamental results of the present study.

Spectroscopic Characterizations of Cu/O_2 1:1 and 2:1 Adducts. (A) Oxygenation Reaction of $[(TMPA)Cu(RCN)]^+$ (1a). Complete spectra between 360 and 750 nm were collected with the setup described in the Experimental Section. Upon rapid mixing of solutions of O_2 and $[(TMPA)Cu(RCN)]^+$ (**1a**), temperature-dependent UV–vis spectral changes occur. Experimental spectra for the oxygenation reaction of $[(TMPA)Cu(RCN)]^+$ at –90 °C are shown in Figure 1.

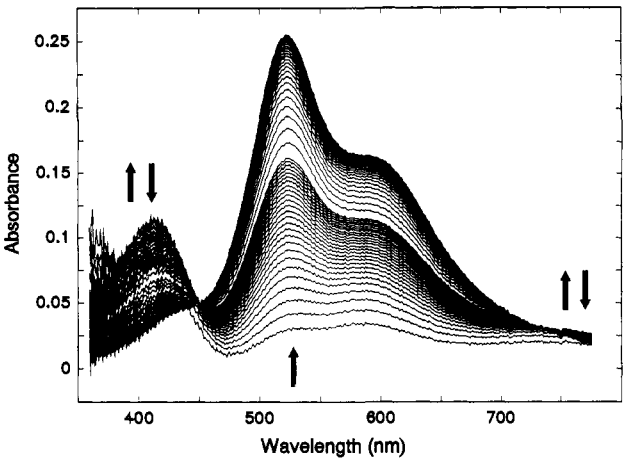

Figure 1. Time-dependent (1 s total), low-temperature UV–vis spectra for the oxygenation reaction of $[(TMPA)Cu(RCN)]^+$ (2.25×10^{-4} M) at –90 °C. $[O_2] = 4.4 \times 10^{-3}$ M.

Between –90 and –75 °C, there is a rapid formation of species **1b** with λ_{max} at 410 and 747 nm; this quickly decays and is transformed into the final stable complex **1c** having 525- and 595- (sh) nm absorptions. Above –70 °C, the rate of formation of species **1b** is beyond the instrumental limit, whereas its thermodynamic stability decreases with increasing temperature. Above –50 °C, formation of **1c** is also incomplete. In addition, irreversible decay to secondary products becomes significant, and the **1b** intermediate is reduced to steady-state concentration at the highest temperatures. For this condition, the formation of the final product **1c** in reaction Scheme I can be described by a single reaction step with an apparent third-order rate constant k_{ter} (M^{-2} s^{-1}) = k_1k_2/k_{-1}.

$$2\underset{\mathbf{1a}}{[LCu^I(RCN)]^+} + O_2 \underset{k_{-2}}{\overset{k_{ter}}{\rightleftharpoons}} \underset{\mathbf{1c}}{[(LCu)_2(O_2)]^{2+}} \qquad (4)$$

$$\frac{d[(LCu)_2(O_2)]^{2+}}{dt} = \frac{k_1k_2}{k_{-1}}[LCu^I]^2[O_2] = k_{ter}[LCu^I]^2[O_2] \qquad (5)$$

The overall data analysis provides the calculated spectrum for the 2:1 adduct $[\{(TMPA)Cu\}_2(O_2)]^{2+}$ (**1c**) with the spectroscopic features λ_{max} = 525 nm and $\epsilon = 1.5 \times 10^4$ M^{-1} cm^{-1} (Figure 2). The calculated spectrum of **1c** agrees very well with that recorded under "synthetic" conditions, i.e., where **1a** is subjected to O_2 bubbling at –80 °C. **1c** is essentially fully formed and stable for hours as observed by UV–vis spectrometry.[33,56] The 525-nm band along with the 440- (sh) and 600-nm (sh) features has been assigned to peroxo to Cu(II) LMCT transitions.[34] In addition to the dinuclear peroxo complex, the numerical analysis permits calculation of the spectrum of the thermodynamically unstable 1:1 adduct $[\{(TMPA)Cu\}(O_2)]^+$ (**1b**) with λ_{max} = 410 nm and $\epsilon = 4 \times 10^3$ M^{-1} cm^{-1} (Figure 3). This might best be thought of as a superoxo Cu(II) species, and we speculate the 410-nm absorption may again be a LMCT transition. This is the first case for which the stepwise binding of O_2 to one and subsequently two copper moieties could be directly studied and the spectroscopic characterization as well as kinetic and thermodynamic data for both the 1:1 CuO_2 and 2:1 Cu_2O_2 copper–dioxygen adducts could be obtained.

(55) Karlin, K. D.; Cruse, R. W.; Gultneh, Y.; Farooq, A.; Hayes, J. C.; Zubieta, J. *J. Am. Chem. Soc.* **1987**, *109*, 2668–2679.

(56) Tyeklár, Z.; Karlin, K. D. *Acc. Chem. Res.* **1989**, *22*, 241–248.

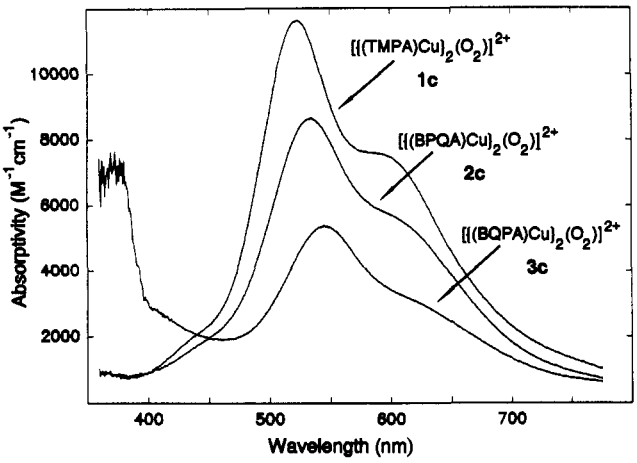

Figure 2. Calculated spectra for the dinuclear Cu_2O_2 adducts **1c**, **2c**, and **3c**.

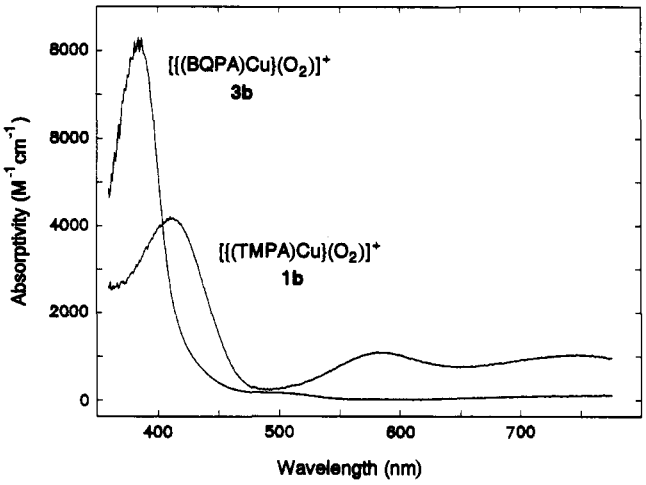

Figure 3. Calculated spectra for the mononuclear CuO_2 adducts **1b** and **3b**.

(B) Oxygenation Reaction of [(BPQA)Cu]$^+$ (2a). Upon rapid mixing of solutions of O_2 and [(BPQA)Cu]$^+$ (**2a**), UV–vis spectral changes occurred, and the spectra of the oxygenated species were recorded. The data reduction and analysis described in the Experimental Section show that only the 2:1 adduct [{(BPQA)-Cu}$_2$(O$_2$)]$^{2+}$ (**2c**) is observed, possessing an absorption with λ_{max} at 535 nm and a shoulder at 600 nm. No mononuclear 1:1 adduct or any other intermediate is detected under the experimental conditions. Thus, the formation of the final product **2c** can be described by a simple one-step reaction with an apparent third-order rate constant k_{ter} (M^{-2} s^{-1}) = k_1k_2/k_{-1} at all temperatures. Time-dependent, low-temperature UV–vis spectra describing the formation of **2c** are shown in Figure 4.

The spectral pattern for the oxygenation process of **2a** is similar to that of **1a**, except for the missing intermediate 1:1 adduct prior to the formation of **2c**. Complete data analysis provides the spectrum of **2c**, with ϵ(535 nm) = 8.6 × 10^3 M^{-1} cm^{-1}, again similar to that observed under the synthetic conditions[44] (Figure 2). It is evident that both **1c** and **2c** are very similar, except that **2c** has somewhat lower molar extinction coefficients accompanied by a small but significant bathochromic shift of the main band. This suggests they both have the same peroxo dicopper(II) binding structure, i.e., a *trans*-μ-1,2-peroxo dicopper(II) ligation.

(C) Oxygenation Reaction of [(BQPA)Cu]$^+$ (3a). Upon rapid mixing of solutions of O_2 and [(BQPA)Cu]$^+$ (**3a**), temperature- and concentration-dependent UV–vis spectral changes occurred. At –90 °C, we observed the rapid formation and decay of a species with λ_{max} at 545 nm accompanied by the formation of another species with λ_{max} at 378 nm. The maximum absorbance observable

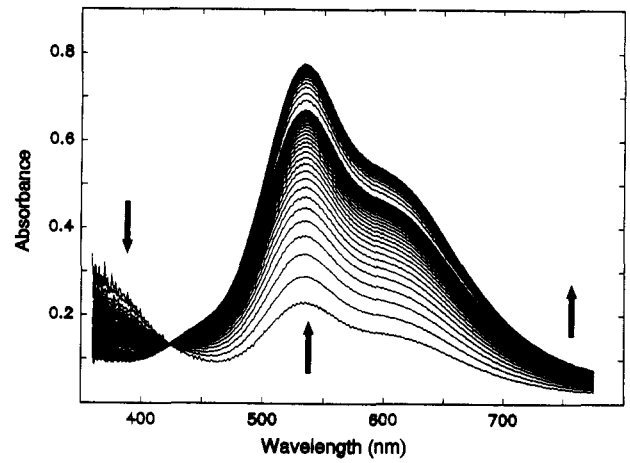

Figure 4. Time-dependent (1 s total), low-temperature UV–vis spectra for the oxygenation reaction of [(BPQA)Cu]$^+$ (9.57 × 10^{-4} M) at –50 °C. [O_2] = 4.4 × 10^{-3} M.

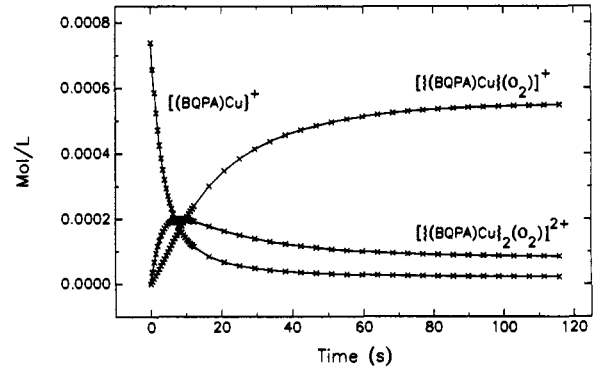

Figure 5. Concentration changes of species **3a**–**3c** as a function of time at –90 °C.

for the 545-nm band is sensitive to the temperature and the concentration of Cu(I). On the basis of complete calculations of data collected with variable Cu(I) concentrations and temperatures using the reaction mechanism outlined in Scheme I, it is concluded that the initially formed species is the thermodynamically unstable 2:1 adduct [{(BQPA)Cu}$_2$(O$_2$)]$^{2+}$ (**3c**, ϵ(545 nm) = 5.5 × 10^3 M^{-1} cm^{-1}) and the final stable species with λ_{max} = 378 nm is the 1:1 adduct [{(BQPA)Cu}(O$_2$)]$^+$ (**3b**, ϵ(378 nm) = 8 × 10^3 M^{-1} cm^{-1}). The [(BQPA)Cu]$^+$ complex thus preferentially forms a 1:1 adduct, [{(BQPA)Cu}(O$_2$)]$^+$ (**3b**), and only a small amount of the 2:1 copper–peroxo complex [{(BQPA)-Cu}$_2$(O$_2$)]$^{2+}$ (**3c**) is initially observed. There exists an "overshooting" in the reaction of **3a** with dioxygen, i.e., the 2:1 adduct **3c** forms rapidly as long as an excess of free unoxygenated complex [(BQPA)Cu]$^+$ is present, which then converts to the thermodynamically stable complex **3b** concomitant with the essentially complete consumption of Cu(I). Presumably, the significant suppression of the formation of the 2:1 adduct **3c** is due to steric hindrance. A plot of concentration change vs time for each individual species involved in the oxygenation reaction of **3a** at –90 °C is shown in Figure 5. From this, we can see that the Cu(I) concentration decreases nearly to completion upon Cu(I) reacting with dioxygen, while the concentration of the CuO_2 1:1 adduct steadily increases. The concentration rise and fall of [{(BQPA)Cu}$_2$(O$_2$)]$^{2+}$ are also apparent from an examination of Figure 5. Calculated spectra for **3c** and **3b** are shown in Figures 2 and 3, respectively. Again, the calculated spectrum for **3b** is almost identical to that observed in a low-temperature UV–vis study under synthetic conditions in which a 1:1 [(BQPA)Cu]$^+$:O_2 stoichiometry was also established;[44] again, the strong band at 378 nm is tentatively assigned as an O_2^- to Cu(II) LMCT transition.[44]

Table I. Kinetic Parameters for O_2-Interaction with Copper(I) Complexes **1a–3a**[a]

parameter		[(TMPA)Cu(RCN)]$^+$ (**1a**)	[(BPQA)Cu]$^+$ (**2a**)	[(BQPACu]$^+$ (**3a**)
k_1 (M^{-1} s^{-1})	183 K	$(1.8 \pm 0.1) \times 10^4$		18 ± 1
	298 K	8×10^7 [b]		6×10^4 [b]
$\Delta H^{\ddagger}$ (kJ mol^{-1})		32 ± 4		30 ± 2
$\Delta S^{\ddagger}$ (J K^{-1} mol^{-1})		14 ± 18		-53 ± 8
k_{-1} (s^{-1})	183 K	8 ± 1		$(6.1 \pm 0.7) \times 10^{-3}$
	298 K	2×10^8 [b]		2×10^5 [b]
$\Delta H^{\ddagger}$ (kJ mol^{-1})		66 ± 4		65 ± 4
$\Delta S^{\ddagger}$ (J K^{-1} mol^{-1})		137 ± 18		72 ± 19
k_2 (M^{-1} s^{-1})	183 K	$(3.2 \pm 0.2) \times 10^4$		
	298 K	$(1.8 \pm 0.1) \times 10^6$		
$\Delta H^{\ddagger}$ (kJ mol^{-1})		14 ± 1		
$\Delta S^{\ddagger}$ (J K^{-1} mol^{-1})		-78 ± 2		
k_{-2} (s^{-1})	183 K	$(1.5 \pm 0.8) \times 10^{-4}$	$(1.9 \pm 0.3) \times 10^{-4}$	
	298 K	$(1.2 \pm 0.3) \times 10^3$	$(1.6 \pm 0.2) \times 10^3$	
$\Delta H^{\ddagger}$ (kJ mol^{-1})		61 ± 3	61 ± 1	
$\Delta S^{\ddagger}$ (J K^{-1} mol^{-1})		19 ± 10	21 ± 4	
k_{ter} (M^{-2} s^{-1})	183 K	$(6.2 \pm 0.5) \times 10^7$	$(3.2 \pm 0.1) \times 10^6$	
	298 K	$(6 \pm 1) \times 10^5$	$(6.8 \pm 0.4) \times 10^5$	
$\Delta H^{\ddagger}$ (kJ mol^{-1})		-20 ± 2	-8 ± 1	
$\Delta S^{\ddagger}$ (J K^{-1} mol^{-1})		-201 ± 5	-160 ± 2	

[a] Standard errors of rate constants were calculated from the results of the linear regression analyses for the corresponding activation parameters. Rate constants at intermediate temperatures would therefore automatically have smaller associated errors than those at the extreme values of 183 and 298 K. [b] Relatively uncertain values extrapolated from activation parameters based exclusively on low-temperature data. Calculated uncertainties are close to a factor of 2 (4 for k_{-1}).

Table II. Thermodynamic Parameters for O_2-Interaction with Cu(I) Complexes 1a–3a

parameter		[(TMPA)Cu(RCN)]$^+$ (**1a**)	[(BPQA)Cu]$^+$ (**2a**)	[(BQPACu]$^+$ (**3a**)
K_1 (M^{-1})	183 K	$(1.9 \pm 0.1) \times 10^3$		$(2.9 \pm 0.3) \times 10^3$
	298 K	0.34 ± 0.08		0.4[a]
$\Delta H°$ (kJ mol^{-1})		-34 ± 1		-35 ± 6
$\Delta S°$ (J K^{-1} mol^{-1})		-123 ± 4		-125 ± 27
K_2 (M^{-1})	183 K	$(2.2 \pm 0.7) \times 10^8$		$(2.0 \pm 0.2) \times 10^3$
	298 K	$(1.5 \pm 0.4) \times 10^3$		40[a]
$\Delta H°$ (kJ mol^{-1})		-47 ± 3		-15[b]
$\Delta S°$ (J K^{-1} mol^{-1})		-97 ± 10		-20[b]
$\beta_2 = K_2K_2$ (M^{-2})	183 K	$(4.3 \pm 1.5) \times 10^{11}$	$(1.7 \pm 0.2) \times 10^{10}$	$(6 \pm 1) \times 10^6$
	298 K	$(5 \pm 1) \times 10^2$	$(4.4 \pm 0.6) \times 10^2$	20[a]
$\Delta H°$ (kJ mol^{-1})		-81 ± 3	-69 ± 2	-50[b]
$\Delta S°$ (J K^{-1} mol^{-1})		-220 ± 11	-181 ± 5	-145[b]

[a] Extrapolated values known within a factor of 2–4 only. [b] Values based on the 183 K value of K_2 and an ill-defined temperature dependence.

(D) Oxygenation Reaction of [(TMQA)Cu]$^+$ (4a). **4a** does not react with dioxygen, and thus a kinetic study was not possible. We suggest that this lack of reactivity is due to both steric hindrance and electronic effects. The $E_{1/2}$ for **4a** as measured by cyclic voltammetry is –0.24 V vs Ag/Ag^+ in DMF solvent, a value which is significantly more positive than that found for **1a–3a** (–0.61 to –0.41 V). These factors are discussed further elsewhere.[44]

(E) Spectral Comparison of Cu/O_2 1:1 and 2:1 Adducts. One-to-one CuO_2 copper dioxygen adducts are of great interest[44] because they are of fundamental importance in Cu/O_2 reactivity of both chemical and biological origin. Following our initial communication,[30] this study describes the first spectral as well as kinetic/thermodynamic (vide infra) descriptions for CuO_2 complexes. We note here that **1b** and **3b** exhibit similar spectroscopic features, although the differences in λ_{max} and molar extinction coefficients suggest that the variation in ligand affects the electronic properties of the CuO_2 moiety, too. Increasing quinolyl ligand substitution in the 1:1 complexes exerts a remarkable hypsochromic shift of λ_{max} from 410 to 378 nm accompanied by a 2-fold increase in molar absorptivity. Clearly, details of ligand design are crucial, and additional studies will be needed to determine the actual structure of these species.

From Figure 2, we see that the three spectra for the 2:1 adducts **1c–3c** are quite similar, all having prominent charge-transfer peaks around 500–550 nm with a characteristic shoulder at lower energies. There is a bathochromic shift from 525 to 545 nm and a concomitant decrease in the molar extinction coefficients from 1.5×10^4 to 5.5×10^3 M^{-1} cm^{-1} with increased quinolyl ligand substitution. On the basis of the UV–vis spectra of these 2:1 adducts, we assume that all these species have the same *trans*-μ-peroxo dicopper(II) binding as that seen in $[\{(TMPA)Cu\}_2(O_2)]^{2+}$. The opposite trends in λ_{max} and molar absorptivities for the 1:1 and 2:1 adducts upon increasing quinolyl substitution may point to a different origin of the respective main bands. This should, however, be considered as an open question at present, pending a larger body of experimental data and/or detailed quantum-mechanical assignment of the respective bands.

Kinetic and Thermodynamic Parameters for Copper(I) Complexes 1a–3a. With respect to kinetic and thermodynamic parameters for dioxygen interaction, the three copper(I) complexes also show many similarities, even though increased quinolyl substitution and consequent steric hindrance have some major effects. Factors that could have an effect on both types of parameters would include electronic and steric influences as well as possible differences in solvent ligation. These could not be generally disentangled in the present study and are individually referred to in some obvious cases only. The relevant activation enthalpies and entropies are shown in Table I, together with the individual rate constants calculated for 183 and 298 K.

By combination of the appropriate kinetic parameters for the corresponding forward and backward reactions or by direct analysis of rapidly playing equilibria, cf. Experimental Section, thermodynamic parameters have also been derived. Reaction enthalpies and entropies are collected in Table II. Of course, kinetic and thermodynamic values are not independent.[57] Minor numerical inconsistencies are due to rounding errors.

(A) Formation and Dissociation of the 1:1 adduct. As shown in Table I, activation enthalpies for k_1 and k_{-1} (initial on and off O_2-reaction, Scheme I) are identical within experimental error for the systems that can be compared, i.e., $[(TMPA)Cu(RCN)]^+$ (**1a**) and $[(BQPA)Cu]^+$ (**3a**). In other words, the enthalpic parts for both formation and dissociation of the 1:1 adducts with **1a** and **3a** are nearly identical. The considerably smaller values of k_1 observed for **3a** are exclusively due to the less favorable entropy term (−53 J K^{-1} mol^{-1} for **3a** vs 14 J K^{-1} mol^{-1} for **1a**). One factor which could contribute to the large difference in $\Delta S^{\ddagger}$ may be that there is a loss of coordinated RCN for **1a** upon O_2-binding (Scheme I, eq 1). Solvent ligation may have different characteristics in **1a** and **3a**, as indicated by the absence of RCN in $[(BQPA)Cu]^+$ crystals,[44] although its coordination in solution is strongly indicated by UV–vis spectra for all complexes.[58]

Whatever the influence of coordination or noncoordination of the additional nitrile ligand, this does not significantly affect the overall stability of the 1:1 adducts $[LCu(O_2)]^+$, since reaction enthalpies (−34 or −36 kJ mol^{-1}) as well as reaction entropies (−123 or −125 J K^{-1} mol^{-1}) are identical within experimental error for O_2-interaction with **1a** and **3a**, respectively. It thus seems equally appropriate to assume that the overall process of both reactions is closely related and to attribute the decreased rates with **3a** to geometric hindrance by the bulkier quinoline groups.

For **2a**, the 1:1 adduct has not been detected under any experimental conditions. Most likely this is not due to the intrinsic instability of that species but rather due to rapid further reaction to give the 2:1 adduct. This is in accord with the extremely fast formation observed for **3c**. The reason for observing the 1:1 adduct in the $[(BQPA)Cu]^+$ system is due to the relative thermodynamic instability of **3c** which is only seen as an "intermediate"; $[\{(BQPA)Cu\}(O_2)]^+$ is the ultimate thermodynamic sink. Despite our lacking experimental evidence for the $[(BPQA)Cu]^+$ system, we think that the three 1:1 adducts would have roughly the same equilibrium constants.

We note that according to measured reduction potentials of **1a** vs **3a** ($E_{1/2}$ = −0.61 and −0.41 V in DMF vs $Ag/AgNO_3$, respectively),[44] one might expect K_1 (Table II) to be greater for **1a**, with its greater driving force for oxidation of Cu(I) to Cu(II).[7,10] As this is not the case, the subtleties of differences in the ligand of steric hindrance and/or coordination geometry might be contributing to the overall binding stabilities of the 1:1 CuO_2 adducts.

(B) Formation and Dissociation of the 2:1 Adduct. As shown in Table I, activation enthalpies for k_{-2} are identical for **1c** and **2c**, i.e., for the systems that can be compared. Interestingly, activation enthalpies for dissociation are all in the narrow range of 61–66 kJ mol^{-1}, independent of the ligand and whether relating to the 1:1 (k_{-1}) or 2:1 (k_{-2}) species. It is unfortunate that the rate constants of **3a** for the second step (Scheme I) where $[\{(BQPA)Cu\}(O_2)]^+$ reacts with $[(BQPA)Cu]^+$ could not be obtained. Despite the relative thermodynamic instability of the 2:1 adduct $[\{(BQPA)Cu\}_2(O_2)]^{2+}$ (**3c**), this equilibrium is always established much faster than the formation of the 1:1 adduct, and therefore, only equilibrium data were obtained[59] for the dimeric peroxo dicopper(II) species **3c**.

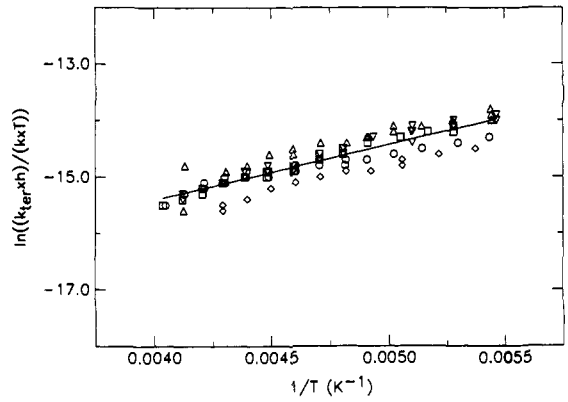

Figure 6. Plot of $\ln[(k_{ter}h)/(\kappa T)]$ vs $1/T$. $[(BPQA)Cu]^+/[O_2]$: △, 9.57 × 10^{-4} M/4.4 × 10^{-3} M; ○, 6.40 × 10^{-4} M/4.4 × 10^{-3} M; □, 5.24 × 10^{-4} M/4.4 × 10^{-3} M; ◇, 2.02 × 10^{-4} M/4.4 × 10^{-3} M; and ▽, 6.59 × 10^{-4} M/9.24 × 10^{-4} M.

As shown in Table I, the overall forward reaction to form the 2:1 adduct described by k_{ter} exhibits a negative activation enthalpy and a highly negative activation entropy for both **1a** and **2a**. Consequently, the rate of 2:1 adduct formation decreases with increasing temperature. This fact can also be seen from the $\ln[(k_{ter}h)/(\kappa T)]$ vs $1/T$ plot for the **2a** system (Figure 6). This plot was generated by simultaneous linear regression for five series of measurements for **2a**. The large negative intercept of the plot reflects the large negative activation entropy, and the positive slope describes the negative activation enthalpy. This negative $\Delta H^{\ddagger}$ for k_{ter} is, of course, due to the preequilibrium constant $K_1 = k_1/k_{-1}$, which significantly decreases with increasing temperature.

Whereas thermodynamic stability is hardly affected at all for the 1:1 $[LCu(O_2)]^+$ species by increasing steric hindrance, quinoline-for-pyridyl substitution has a remarkable effect on the dinuclear $[(LCu)_2(O_2)]^{2+}$ adducts. Reaction enthalpies decrease from −81 (TMPA) to −69 (BPQA) to −50 (BQPA) kJ mol^{-1} for the overall formation constant $\beta_2 = K_1K_2$ of **1c–3c**. In line with the relatively minor effects on k_{ter} and k_{-2} for $[(TMPA)Cu]^+$ and $[(BPQA)Cu]^+$, the decrease in thermodynamic stability is more pronounced in going from **2a** to **3a** than upon substitution of the first pyridyl group. Obviously, two quinoline groups per ligand are too demanding sterically to allow efficient simultaneous binding of two complex moieties to the same dioxygen molecule. The involvement of steric rather than electronic effects for the observed differences is strongly supported by the close spectral resemblance and the practical identity of 1:1 adduct stabilities discussed above. It should be noted here that K_2 and consequently β_2 obtained at 183 K are the primary reliable data for $[(BQPA)Cu]^+$, whereas the temperature dependence of this parameter could only be followed between 183 and 193 K. The corresponding reaction enthalpies and entropies are hardly more than educated guesses. This, however, has no influence on the main statement of the reduced stability of **3c**.

The rate constants listed in Table I reflect the trends in the activation parameters just discussed. We observed that (a) the rate constants k_1 and k_{-1} for **1a** and **3a** have a similar temperature dependence; they are slower in the latter system by several orders of magnitude, which might be related to the bulkier ligand environment in **3a** relative to that in **1a**; (b) the dissociation is always more favored at higher temperatures than the association for **1a–3a**; and (c) the rate of overall formation decreases with increasing temperature.

From the thermodynamic parameters in Table II, we see that all equilibrium constants decrease with increasing temperature, as all equilibria are driven by negative reaction enthalpies and destabilized at higher temperatures by unfavorable entropy terms.

(57) Theoretically, equilibrium and kinetic data are strictly correlated, e.g., $K_1 = k_1/k_{-1}$. Numerical inconsistencies between Tables I and II are due to rounding errors and to different bases for the linear regressions. The latter arises from the fact that equilibrium values were partly calculated by the combination of the appropriate kinetic parameters and partly obtained directly from spectral analysis, cf., Experimental Section, Data Reduction Methods.

(58) In EtCN solvent, complexes **2a–4a** show the same UV–vis spectral pattern. However, **4a** exhibits a very different spectrum in RCN compared to in CH_2Cl_2, indicative of the coordination of EtCN with the Cu(I) center. (Note: complexes **2a** and **3a** are not stable in CH_2Cl_2, since they react with this solvent.) By analogy, EtCN also interacts with **2a** and **3a**.

(59) Using low values for k_2 and k_{-2} resulted in unacceptable overall fit and/or spectra. When k_2 and k_{-2} were increased over a certain limit, spectra and fit became reasonable and depended on the ratio $k_2/k_{-2} = K_2$ only.

Table III. Kinetic and Equilibrium Constants for O_2-Binding at Room Temperature

system	k_1 (O_2) (M^{-1} s^{-1})	K_1 (M^{-1})
Mb (sperm whale)[71]	2.3×10^7	9.7×10^5
Hb (hemoglobin), R state[87]	3×10^7	2×10^6
Hb (hemoglobin, T state[87]	7×10^7	5×10^4
picket-fence, R state[88]	4.3×10^3	1.5
Picket-fence, T state[88]	1.1×10^8	2.4×10^3
pocket-picket, R state[88]	2.2×10^6	2.4×10^5
chelated heme[89]		
short tail	4.6×10^7	3.1×10^5
medium tail	2.2×10^7	9.6×10^5
long tail	2.9×10^7	1.2×10^6
strapped heme[90]		
tight strap	3×10^5	
loose strap	1.7×10^6	6.8×10^3
Cu(I) mononuclear complexes (this work)	(6×10^4) – (8×10^7)	0.3–0.4
cytochrome *c* oxidase[69,70]	3.5×10^8	7.0×10^3
LCo^{2+} (L = C-*meso*-Me_6[14]aneN$_4$)[91]		
LCo^{2+}	5.0×10^6	301
$(Cl)LCo^{2+}$	1.8×10^6	560
$[Co(l\text{-histidinato})_2]^{2+}$ [67]	3.5×10^3	
hemerythrin (Hr) (octamer P.g.)[a,71]	1.2×10^7	2.8×10^5
hemocyanin (Hc) (monomer P.i.)[a,71]	5.7×10^7	5.7×10^5
hemocyanin (Hc) (hexamer P.i.)[a,72]	3.1×10^7	5.2×10^5
hemocyanin (monomer subunit a, P.i.)[a,95]	4.6×10^7	1.1×10^5
$[Cu_2XYL\text{–}H]^{2+}$ [a,31]	4570 (20 °C)	6
$[Cu_2XYL\text{–}O\text{–}]^{+}$ [a,31]	$>10^6$ (–80 °C)	35 (25 °C)

[a] M_2O_2 is formed during the oxygenation reaction. P.g., *Phascolopsis gouldii*; P.i., *Panulirus interruptus*.

Comparison of Copper/O_2 Kinetic/Thermodynamic Parameters with Other Metal Complexes and Proteins. Cobalt complexes are capable of binding dioxygen to form either 1:1 and/or 2:1 adducts.[7,8,10] The dinuclear peroxo dicobalt(III) complexes are generally more stable than the 1:1 adducts and will be formed unless inhibited sterically (such as in vitamin B_{12},[60,61] coboglobins,[10,62] and cobalt porphyrins[63,64]) or by the combined use of low temperature, low concentration, and nonaqueous solvents (to inhibit formation of a more highly charged dimer).[7] The presence of 1:1 CoO_2 was supported by fast kinetic studies, and the LCo/O_2 reaction mechanism (the same as for the $[LCu]^+/O_2$ reaction) was originally deduced by Wilkins and co-workers.[65–67] Today, there are many stable and isolable 1:1 CoO_2 complexes best described as Co(III)–O_2^- species,[1,2,7,10] and some of these have been characterized by X-ray crystallography.[7,68] Most of them have an end-on (i.e., terminal η^1) Co–O_2^- structure, although one example of a side-on η^2 superoxo Co(III) complex has been confirmed.[68] Either structure would seem possible for Cu(II)–O_2^-, at this early stage of our understanding. Comparing the mononuclear $[LCu]^+$ with cobalt(II) complexes in reaction with dioxygen, we observed that the formation rates are comparable but that the equilibrium constants are about 100 times less for 1:1 CuO_2 complexes at room temperature (Table III). This suggests an effect ascribable to the off-rate k_{-1}, i.e., O_2^- is more tightly bound to Co(III) than Cu(II).

In the absence of sufficient data based on activation parameters and reaction enthalpies as well as entropies, the reason for higher room-temperature stabilities of cobalt–dioxygen adducts is not easily discussed. It must always be kept in mind, however, that low spin Co(III) rather than Cu(II) is a chemically inert species, and for this reason alone, k_{-1} values will basically be smaller for Co–dioxygen adducts.

It is also of interest to compare the kinetic and thermodynamic parameters for the formation of the 1:1 CuO_2 adducts **1b** and **3b** with proteins and other synthetic model systems which form O_2-complexes with the same stoichiometry. Hemoglobin, myoglobin, and certain porphyrin–iron model complexes are known to form stable 1:1 FeO_2 complexes. There is also recent spectral evidence and kinetic data indicating that when reduced cytochrome *c* oxidase (*Cc*O) reacts with dioxygen, a transient Cu–O_2 adduct forms in the initial reaction with the dinuclear cyt a_3–Cu_B site.[69,70] For the copper–dioxygen carrier protein hemocyanin (Hc), however, there is no spectral and kinetic/thermodynamic information reported for 1:1 CuO_2 formation, and only direct addition to the dinuclear copper center is observed.[71,72,95] This is interesting, since the recent X-ray structure of deoxy-Hc from *Limulus polyphemus* shows that Cu(I)···Cu(I) = 4.6 Å,[18] suggesting that a 1:1 CuO_2 adduct may very well initially form. Copper–dioxygen 1:1 complexes have long been proposed as intermediates present in Cu(I) autoxidation processes[73] and in the reaction of Cu(II)-(aq) or other Cu(II) complexes with superoxide ion.[74–83] Copper-(II)–superoxide species have also been obtained by reacting O_2 with a Cu(I) mononuclear[84,85] or Cu(II)Cu(I) mixed-valence dinuclear complex.[86] However, the present study provides the first kinetic and thermodynamic data for 1:1 CuO_2 adduct formation.

From Table III, we can see that for copper(I) complexes, the rate constants k_1 at room temperature (extrapolated, Table II) for the formation of the CuO_2 1:1 adducts (10^5–10^8 M^{-1} s^{-1}) are comparable with those for iron proteins Hb/Mb as well as porphyrin–iron model complexes (generally in the range of 10^5–10^8 M^{-1} s^{-1}). However, the equilibrium constants K_1 (0.3–0.4 M^{-1}) for CuO_2 formation are dramatically smaller than those for iron proteins and model complexes, due to the large off-rate k_{-1} associated with our copper model complexes. The same appears to be true for cytochrome *c* oxidase, where flash-flow methods give kinetic data for Cu_B–O_2 formation, $k_1 \simeq 10^8$ M^{-1} s^{-1} and $K_1 \simeq 7000$ M^{-1}. These observations may indicate an extra stabilization of the O_2^- bond to copper in *Cc*O relative to those in model complexes **1b** and **3b**, but again, it is impossible presently to attribute this extra stabilization to a specific reason such as

(60) Schrauzer, G. N.; Lee, L. P. *J. Am. Chem. Soc.* **1970**, *92*, 1551.
(61) Bayston, J. H.; King, N. K.; Looney, F. D.; Winfield, M. E. *J. Am. Chem. Soc.* **1969**, *91*, 2775.
(62) Tauzher, G.; Amiconi, G.; Antonini, E.; Brunori, M.; Costa, G. *Nature (London)* **1973**, *241*, 222.
(63) Walker, F. A.; Beroiz, D.; Kadish, K. M. *J. Am. Chem. Soc.* **1976**, *98*, 3484.
(64) Collman, J. P.; Brauman, J. I.; Halber, T. R.; Suslick, K. S. *Proc. Natl. Acad. Sci. U.S.A.* **1976**, *73*, 3333.
(65) Wilkins, R. G. *Adv. Chem. Ser.* **1971**, *100*, 111.
(66) Miller, F.; Simplicio, J.; Wilkins, R. G. *J. Am. Chem. Soc.* **1969**, *91*, 1962–1967.
(67) Simplicio, J.; Wilkins, R. G. *J. Am. Chem. Soc.* **1967**, *89*, 6092–6095.
(68) Egan, J. W., Jr.; Haggerty, B. S.; Rheingold, A. L.; Sendlinger, S. C.; Theopold, K. H. *J. Am. Chem. Soc.* **1990**, *112*, 2445–2446.
(69) Blackmore, R. S.; Greenwood, C.; Gibson, Q. H. *J. Biol. Chem.* **1991**, *266*, 19245–19249.
(70) Oliveberg, M.; Malmström, B. G. *Biochemistry* **1992**, *31*, 3560–3563.
(71) Armstrong, G. D.; Sykes, A. G. *Inorg. Chem.* **1986**, *25*, 3135–3139.
(72) Kuiper, H. A.; Antonini, E.; Brunori, M. *J. Mol. Biol.* **1977**, *116*, 569–576.
(73) Zuberbühler, A. D. In *Metal Ions in Biological Systems*; Sigel, H., Ed.; Marcel Dekker: New York, 1976; Vol. 5; pp 325–368.
(74) Meisel, D.; Levanon, H.; Czapski, G. *J. Phys. Chem.* **1974**, *78*, 779–782.
(75) Czapski, G.; Goldstein, S.; Meyerstein, D. *Free Radical Res. Commun.* **1988**, *4*, 231–236.
(76) Goldstein, S.; Czapski, G. *Free Radical Res. Commun.* **1991**, *12–13*, 205–210.
(77) Strothkamp, K. G.; Lippard, S. J. *Acc. Chem. Res.* **1982**, *15*, 318–326.
(78) O'Young, C. L.; Lippard, S. J. *J. Am. Chem. Soc.* **1980**, *102*, 4920–4924.
(79) Weinstein, J.; Bielski, B. H. J. *J. Am. Chem. Soc.* **1980**, *102*, 4916–4919.
(80) Roberts, J. L., Jr.; Sawyer, D. T. *Isr. J. Chem.* **1983**, *23*, 430–438.
(81) Tait, A. M.; Hoffman, M. Z.; Hayon, E. *Inorg. Chem.* **1976**, *15*, 934.
(82) Bailey, C. L.; Bereman, R. D.; Rillema, D. P. *Inorg. Chem.* **1986**, *25*, 3149–3153.
(83) Nappa, M.; Valentine, J. S.; Miksztal, A. R.; Schugar, H. G.; Isied, S. S. *J. Am. Chem. Soc.* **1979**, *101*, 7744–7746.
(84) Thompson, J. S. *J. Am. Chem. Soc.* **1984**, *106*, 4057–4059.
(85) Thompson, J. S. In *Biological & Inorganic Copper Chemistry*; Karlin, K. D., Zubieta, J., Eds.; Adenine Press: Guilderland, NY, 1986; Vol. 2, pp 1–10.
(86) Tahir, M. M.; Karlin, K. D. *J. Am. Chem. Soc.* **1992**, *114*, 7600–7601.

additional heme interaction, specific protein influence, or optimized electronic/steric conditions.

Kinetic and thermodynamic data for formation of oxygenated metalloprotein are also available for the dioxygen carrier Hc of arthropods and molluscs and the marine worm iron protein hemerythrin (Hr). These values are listed in Table III as well. It is worthwhile to point out that although the rate constant k_1 and the equilibrium constant K_1 for Hc and Hr proteins have the same units and indicate a two-body collision process as for the 1:1 CuO_2 adduct formation from **1a** and **3a**, these reactions differ in detail from those for the $[LCu]^+$ complexes, since the protein systems are forming 2:1 M_2O_2 adducts. The same is true for the dinuclear complexes $[Cu_2(XYL–H)]^{2+}$ and $[Cu_2(XYL–O–)]^+$, whose O_2-binding kinetics/thermodynamics have been previously described.[31] The rate constants for proteins ($k_1 \simeq 10^5$–10^7 M^{-1} s^{-1}) are in the same range as for **1a** and **3a**, but equilibrium constants K_1 in the latter case are again much smaller. This effect may be protein environment derived but could also be due to the strong binding by two Cu or Fe ions in the O_2 carrier compared to one Cu in **1b** and **3b**. Comparing k_1 for **1a** and **3a** with the dinuclear copper complexes $[Cu_2(XYL–H)]^{2+}$ and $[Cu_2(XYL–O–)]^+$, we see that mono- and dinuclear copper complexes both have large oxygenation on-rate constants but small equilibrium constants K_1.

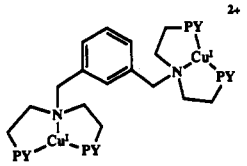

$[Cu_2(XYL\text{-}H)]^{2+}$

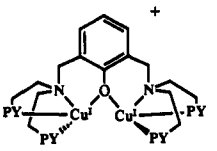

$[Cu_2(XYL\text{-}O\cdot)]^+$

The discussion so far should strongly warn us against comparing kinetic and/or equilibrium data for a single temperature, however. Reaction enthalpies of –81 and –69 kJ mol^{-1} for $[\{(TMPA)Cu\}_2(O_2)]^{2+}$ (**1c**) and $[\{(BPQA)Cu\}_2(O_2)]^{2+}$ (**2c**) are related to a strength in copper–dioxygen binding which compares very favorably with results for dinucleating copper complexes,[31] hemocyanin,[71] or even hemoglobin.[87] Even the reaction enthalpies of roughly –35 kJ mol^{-1} for the 1:1 complexes described in this study are quite significant and in the range of some enzyme data. The reduced overall room-temperature stability of the present dioxygen adducts thus is exclusively due to very unfavorable and, so far, poorly understood entropy terms rather than to factors directly related to bonding strength.

Due to the different molecularity of the reaction of O_2 with mononuclear copper(I) complexes **1a**–**3a** to form the 2:1 Cu_2O_2 adducts as opposed to those of other Cu_2O_2 complexes derived from discrete dinuclear precursors (i.e., $[Cu_2(XYL–H)]^{2+}$ and $[Cu_2(XYL–O–)]^+$), it is not possible to meaningfully compare the rates of formation of the final Cu_2O_2 complexes. However, we can compare the rate constant k_{on} representing the overall formation for Cu_2O_2 with Co(II) systems. We find that k_{on} for **1a** and **2a** at room temperature parallels the values seen for peroxo dicobalt(III) Co_2O_2 complexes analogously derived from mononuclear LCo(II) species (e.g., $k_{on} \simeq (10^8$–$10^9)$ M^{-2} s^{-1} for Co^{2+} complexes of N_4-macrocycles[92]). Co_2O_2 complexes also exhibit large, negative $\Delta S°$ values but still have considerable room-temperature stabilities (log $K_{eq} \simeq 6$–15).[7,8,10,67,93,94] These are derived from much larger, negative $\Delta H°$ values (e.g., ~120–150 kJ mol^{-1})[7,8,10,93,94] for $\beta_2 = K_1K_2$.

Conclusions

In this study, we report the spectral characteristics and full kinetic and thermodynamic results for the formation of the CuO_2 1:1 and Cu_2O_2 2:1 adducts with a series of tetradentate tripodal ligands all having a N_4 set of donor atoms. We found that modifications to the ligands do affect the rates of formation and dissociation of either adduct. With the tris(quinolyl)-substituted ligand TMQA, no interaction with O_2 is observed for steric reasons. In $[(BQPA)Cu]^+$ (**3a**), both k_1 and k_{-1} are reduced by several orders of magnitude compared to those of $[(TMPA)Cu(RCN)]^+$ (**1a**), again likely due to the bulky ligand environment in the former case. The relative preference for the 1:1 adduct of $[\{(BQPA)Cu\}(O_2)]^+$ (**3b**) over that of $[\{(BQPA)Cu\}_2(O_2)]^{2+}$ is also due to a steric effect, i.e., the further reaction of this 1:1 adduct with another $[(BQPA)Cu]^+$ (**3a**) is largely reduced as the ligand environment becomes more crowded. However, the K_1 values for the 1:1 adducts for $[(TMPA)Cu]^+$ (**1a**) and $[(BQPA)Cu]^+$ are practically the same. The decrease of the equilibrium constants with increasing quinolyl substitution for the formation of the Cu_2O_2 2:1 adducts, therefore, is traced to steric hindrance.

The formation of copper–dioxygen adducts formed by the reaction of the copper(I) species with O_2 is kinetically favorable, and on-rates are comparable with protein systems;[31] however, at room temperature, they are thermodynamically unfavored. The formation of copper–dioxygen complexes is always accompanied by strongly negative reaction entropies, $\Delta S°$ around –200 J K^{-1} mol^{-1}. Thus, this is the main reason for the room-temperature instabilities of these copper–dioxygen adducts, as reaction enthalpies compare quite favorably with those of dioxygen adducts stable at ambient temperatures. It is not clear how, exactly, one can overcome this entropy effect in synthetic systems, in the absence of cooperative effects which are or can be present in the large multisubunit proteins. Nevertheless, quasi-reversible interactions of O_2 with cuprous complexes do generally occur and can be studied in detail, even if such adducts are not stable at room temperature.

Acknowledgment. We thank the National Institutes of Health (K.D.K.) and Swiss National Science Foundation (A.D.Z.) for support of this research.

Supplementary Material Available: Drawings of anaerobic sample handling apparatus and DMA interface and listings of the assembler program (8 pages). Ordering information is given on any current masthead page.

(87) Sawicki, C. A.; Gibson, Q. H. *J. Biol. Chem.* **1977**, *252*, 7538–7547.
(88) Collman, J. P.; Brauman, J. I.; Iverson, B. L.; Sessler, J. L.; Morris, R. M.; Gibson, Q. H. *J. Am. Chem. Soc.* **1983**, *105*, 3052–3064.
(89) Geibel, J.; Cannon, J.; Campbell, D.; Traylor, T. G. *J. Am. Chem. Soc.* **1978**, *100*, 3575–3585.
(90) Ward, B.; Wang, C. B.; Chang, C. K. *J. Am. Chem. Soc.* **1981**, *103*, 5236–5238.
(91) Bakac, A.; Espenson, J. H. *Inorg. Chem.* **1990**, *29*, 2062–2067.
(92) Wong, C. L.; Switer, J. A.; Balakrishnan, K. P.; Endicott, J. F. *J. Am. Chem. Soc.* **1980**, *102*, 5511–5518.
(93) Wilkins, R. G. In *Oxygen Complexes and Oxygen Activation by Transition Metals*; Martell, A. E., Sawyer, D. T., Eds.; Plenum: New York, 1988; pp 49–66.
(94) Brouwer, M.; Baker-King, C. *Inorg. Biochem.* **1988**, *34*, 117–133.
(95) Andrew, C. R.; Mckillop, K. P.; Sykes, A. G. *Biochim. Biophys. Acta* **1993**, *1162*, 105–114.